Pathways of photocatalytic gas phase destruction of HD simulant 2-chloroethyl ethyl sulfide

Alexandre V. Vorontsov,[a] Claude Lion,[b] Evgueni N. Savinov,[a,1] and Panagiotis G. Smirniotis [c,*]

[a] *Boreskov Institute of Catalysis, Novosibirsk 630090, Russian Federation*
[b] *Institut de Topologie et de Dynamique des Systèmes de I'Université Paris-7, Upresa 7086, 1, rue Guy-de-la-Brosse, 75005 Paris, France*
[c] *Department of Chemical and Materials Engineering, 497 Rhodes Hall, University of Cincinnati, Cincinnati, OH 45221-0012, USA*

Abstract

Photocatalytic oxidation of HD simulant, 2-chloroethyl ethyl sulfide (CEES), was studied in a specially designed coil and flow photocatalytic reactor by means of GC-MS and FTIR techniques. TiO_2 Hombikat UV 100 photocatalyst was deactivated after a few hours of operation, which was signaled by the appearance of incomplete oxidation products in the reactor effluent and accumulation of incomplete oxidation products on the TiO_2 surface. Complete reactivation of the photocatalyst was achieved by washing the photocatalyst with water. Compared to diethyl sulfide, CEES showed lower reactivity in photocatalytic oxidation and was accumulated on the TiO_2 surface after catalyst deactivation. Without UV irradiation, hydrolysis of CEES proceeded on the TiO_2 surface. Major gaseous products of CEES incomplete photocatalytic oxidation are acetaldehyde, chloroacetaldehyde, SO_2, diethyl disulfide, and chloroethylene. Surface products extracted from the TiO_2 surface with acetonitrile and water include mainly 2-chloroethyl ethyl sulfoxide and ethanesulfinic and ethanesulfonic acids, as well as diethyl di-, tri-, and tetrasulfides mono and disubstituted in the β position with a chlorine or hydroxyl group. While surface monodentate sulfates can be removed upon washing, surface bidentate species stayed on the surface and possibly contribute to the permanent catalyst deactivation.
© 2003 Elsevier Inc. All rights reserved.

Keywords: Chemical warfare agents; Photocatalysis; Catalyst deactivation; Reactivation; Mechanism; Products; Coil reactor

1. Introduction

CWA bis(2-chloroethyl)sulfide also called HD, or mustard gas, is a vesicant and principal component of munitions grade mustard. Its high toxicity is associated with the ability of the SCH_2CH_2Cl group to alkylate proteins and other components of living things. 2-Chloroethyl ethyl sulfide contains this group and effectively simulates HD.

In past years, most research efforts in the field of thioethers photocatalysis were centered on their reactivity in the liquid phase. Several literature reports consider photocatalytic oxidation of thioethers in the liquid phase, mostly in acetonitrile [1–15]. Oxidation usually starts with the formation of thioether radical cations. Further transformations

of thioether radical cations were suggested to follow three routes—oxidation of sulfur, α-C–H bond deprotonation, and C–S bond cleavage [7]. Oxidation of sulfur to form sulfoxides and sulfones was detected in many instances of thioethers and was the only initial way for unsubstituted aromatic heterocyclic compounds in acetonitrile [10,13]. Reaction of thioether radical cations through α-C–H bond deprotonation is speculated to be the route of a direct formation of a carbonyl group at the α carbon atom [8] via peroxyl radical chemistry. The C–S bond cleavage in thioether radical cations produces preferentially thiyl radicals and alkyl cations [5]. Their further reactions are considered responsible for products of sulfinic and sulfonic acids, disulfide, and alcohol [7–9].

Previously, photocatalytic destruction of mustard [2] as well as its simulants 2-chloroethyl ethyl sulfide and 2-chloroethyl methyl sulfide [4] was studied in acetonitrile suspensions of TiO_2. Bis(2-chloroethyl)disulfide and mus-

---

tard sulfoxide were predominantly detected as products in mustard degradation. Corresponding sulfoxides and sulfones were detected in the degradation of the simulants.

Gas-phase photocatalytic oxidation of thioethers has been studied in less detail. However, it may be of higher practical importance because it the has been noted that photocatalytic oxidation in the gas phase is more efficient than in the liquid phase, e.g., for 2-phenethyl-2-chloroethyl sulfide [16]. Since photocatalytic oxidation operates at low temperatures close to ambient, catalyst deactivation can be expected for heteroatomic compounds. It was not detected for low-conversion experiments with dimethyl sulfide [17] and short-term destruction of trimethylene sulfide, propylene sulfide, dimethyl disulfide, and thiophene [18]. The photocatalyst deactivation was clearly notable in prolonged gas-phase degradation of high concentrations of 2-phenethyl-2-chloroethyl sulfide [16], H_2S [19], and diethyl sulfide [20]. A separate FTIR study has demonstrated that the catalyst deactivation in diethyl sulfide oxidation is associated with the accumulation of surface sulfates [21]. Therefore, catalyst reactivation was realized in a reactor with periodic catalyst reactivation by washing with water [22].

The present study continues our efforts on photocatalytic destruction of CWA simulants and was undertaken with the goals

(1) to explore gas-phase photocatalytic mineralization of mustard simulant 2-chloroethyl ethyl sulfide and catalyst reactivation;
(2) to investigate the influence of chlorine on the pathways and reactivities of thioether photocatalytic oxidation in the gas phase; and
(3) to detect surface organic compounds responsible for catalyst deactivation and to suggest a mechanism.

2. Experimental

2.1. Materials

TiO_2 Hombikat UV 100 (Sachtleben Chemie GmbH), which is 100% anatase with a surface area about $340 \ m^2/g$, was used as a catalyst. Purified water was employed for all experiments. Zero-grade air (Wright Bros.) was a base for the reactor feed stream. Air from an air line was passed through drierite (Fisher) in order to prepare air for catalyst drying. Sulfuric acid (Fisher, 98%) was diluted twice before use. Hydrogen peroxide (Fisher, 30%) was diluted to a concentration of 3%. 2-Chloroethyl ethyl sulfide 98% was a product of Fluka. GC-MS analysis showed content of 98.8%. Only compounds with a content much exceeding that in the starting CEES were considered as products in this work. Care should be taken to avoid inhalation and skin contact in experiments with CEES as it is a blister agent and contains a small quantity of real CWA mustard.

2.2. Photocatalytic reactor

The reactor feed stream was prepared by mixing humid and dry air at necessary flow rates and injecting liquid 2-chloroethyl ethyl sulfide at the desired rate with a 7490 Cole–Palmer liquid infusion pump into the stream. The water vapor concentration in the reactor feed was kept at 1900 ppm. Teflon tubing was used for all connections in order to decrease adsorption and decomposition of products. The reactor has the shape of a coil made of a glass tube with an internal diameter of 7 mm and is pictured in detail in an earlier work [22]. Titania photocatalyst was deposited onto its internal surface. The gas stream passed through the interior of the coil. TiO_2 was deposited onto the internal surface of the coil using 20 cycles of washing with aqueous TiO_2 suspension (16 g/L) and drying by passing dehumidified air. The total flux of light entering the reactor was measured using standard ferrioxalate actinometry and was equal to 3.2×10^{-4} E/s.

2.3. Analysis

The feed and effluent of the coil reactor were analyzed with a GC-MS QP5050A (Shimadzu) using a gas-sampling valve. Gaseous and volatile products were separated on a Supel-Q PLOT (30 m, 0.32 mm i.d.) capillary column (Supelco). Heavier products were separated with a XTI-5 (30 m, 0.25 mm i.d.) column (Shimadzu). Volatile products in water and acetonitrile that were used to wash the reactor (referred to throughout the paper as reactor wash) were analyzed by two methods. The first method is headspace solid-phase microextraction (SPME) using 85-µm Carboxen/polydimethylsiloxane Stableflex fibers (Supelco). The extraction temperature was about 70 °C and the extraction time 15 min. The second method employed direct injection of reactor wash into GC-MS. Strong acids in the wash were neutralized by Na_2CO_3 prior to injection. Nonvolatile products in the reactor wash were analyzed using trimethylsilyl derivatization with BSTFA + 1% TMCS reagent (Supelco). Analysis of water wash included evaporation of samples adjusted to pH $\sim$ 7 until dryness, derivatization at about 60 °C for 1 h, and analysis on the GC-MS, and was described in detail elsewhere [23]. Analysis of acetonitrile wash was done by the same method but without evaporation prior to derivatization and without pH adjustment.

Compounds were positively identified only if a search in mass spectral libraries NIST 98 or Wiley (7th ed.) provided similarity above 90%. Many products of chloroethyl ethyl sulfide destruction such as polysulfides and thiosulfonates as well as their hydroxylated and chlorinated derivatives were absent in the GC-MS libraries. Their identification was done manually following fragmentation of the parent molecules in electron impact ionization mode [24].

2.4. FTIR study

For FTIR study on surface changes in deactivation/reactivation of photocatalyst, TiO_2 was suspended in isobutanol using an ultrasonic bath, deposited onto a round BaF_2 plate, and dried. The resultant spot was 2 cm in diameter and uniform and contained about 4 mg of TiO_2. The sample was kept irradiated under 36 W fluorescent UV lamp for 2 days to remove all traces of adsorbed organics. The TiO_2/BaF_2 sample was placed into the flow reactor described in [16]. The reactor was kept at 45 °C and irradiated with a 18 W fluorescent UV lamp. The temperature 45 °C was chosen as mean temperature in the coil reactor. The reactor feed was prepared by injection of CEES into the flow of humidified air containing about 2000 ppm of H_2O to give a CEES concentration 130 ppm and passed through the reactor at flow rate of 21 cm^3/min. At the desired time, the TiO_2/BaF_2 sample was taken from the reactor and placed in a Vector 22 spectrometer (Bruker) for taking transmission spectra. All spectra were registered using 4 cm^{-1} resolution and 50-fold accumulation.

3. Results and discussion

Increasing the quantity of titania photocatalyst from 180 to 310 mg markedly improved the performance of the coil photocatalytic reactor in the destruction of diethyl sulfide [22]. Therefore, the present study was performed with a still higher TiO_2 loading of 620 mg. All the experiments were done over the same photocatalyst. Acetone photocatalytic oxidation at different gas flow rates has previously shown that external mass transfer does not limit the reaction in this reactor [22]. Consequently, the results reflect reaction kinetics.

3.1. Effect of CEES concentration on catalyst deactivation/reactivation

Fig. 1A demonstrates CEES photocatalytic oxidation in the coil reactor at a relatively low feed CEES concentration of 160 ppm. Injection of CEES into the feed stream was started at the beginning of the experiment. Only carbon dioxide and water were detected as the CEES oxidation products in the effluent for about 850 min of reaction. Water adsorbs strongly on TiO_2. Thus, its concentration profile does not reflect the reaction and is not considered in this paper. The carbon dioxide concentration in the reactor effluent gradually increased and approached the stoichiometric value for CEES mineralization according to based on the next reaction

$$CH_3CH_2SCH_2CH_2Cl + 7.5O_2$$
$$\rightarrow 4CO_2 + 3H_2O + H_2SO_4 + HCl. \tag{1}$$
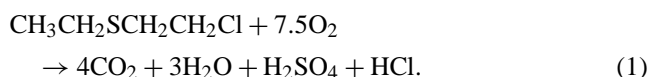
After 850 min of reaction, two products of incomplete oxidation appeared in the effluent—sulfur dioxide and
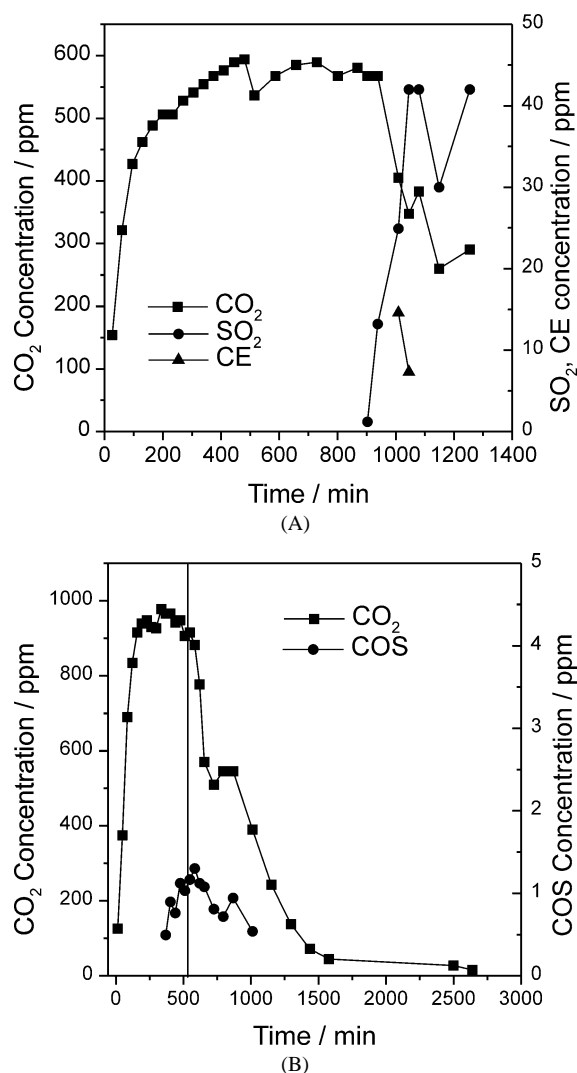

Fig. 1. Reactor effluent concentrations during CEES photocatalytic oxidation. Conditions: CEES injection rate 12 µl/h; feed H_2O concentration 1900 ppm; (A) CEES feed concentration 161 ppm; feed flow rate 260 cm^3/min. CEES injection was turned off at 1035 min. (B) CEES feed concentration 323 ppm; feed flow rate 130 cm^3/min. CEES injection was turned off at 525 min. Product abbreviations are explained in Table 1.

chloroethylene (CE). These products signaled the catalyst deactivation. In order to avoid deep catalyst deactivation, the injection of CEES into the feed stream was stopped at 1035 min. The catalyst stayed irradiated in the flow of humidified air until effluent CO_2 concentration fell to several ppm. The low carbon dioxide concentration meant completion of mineralization of surface organic compounds. Then, the catalyst was washed with five portions of purified water of 100 ml each to remove adsorbed acids. It has been demonstrated previously for diethyl sulfide that irradiation of the photocatalyst in air alone cannot reactivate it to a good extent [22]. Therefore, water washing was a necessary step of the photocatalyst reactivation.

Higher feed concentrations of CEES could result in releasing larger amounts of intermediate products after catalyst deactivation, which is important for detection of prod-
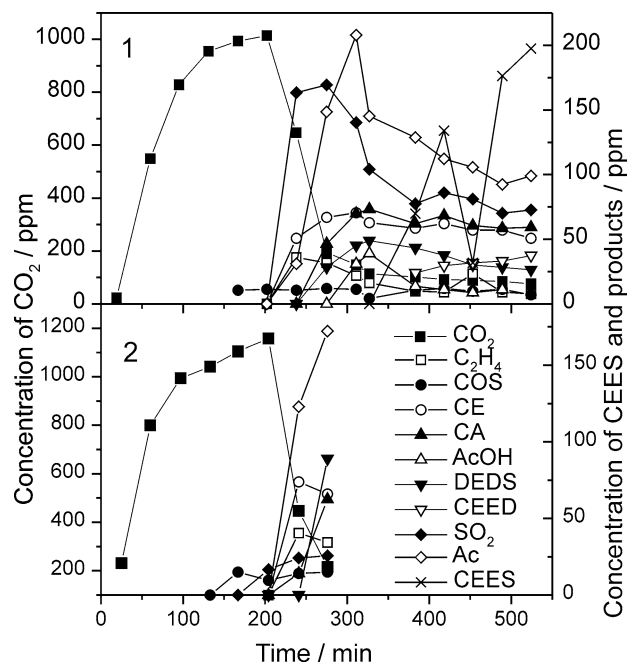
Fig. 2. Profiles of concentrations in the reactor effluent in two consecutive runs of CEES photocatalytic oxidation at CEES feed concentration 404 ppm (30 μl/h liquid CEES), H_2O 1900 ppm, feed flow rate 260 cm^3/min. Product abbreviations are explained in Table 1.
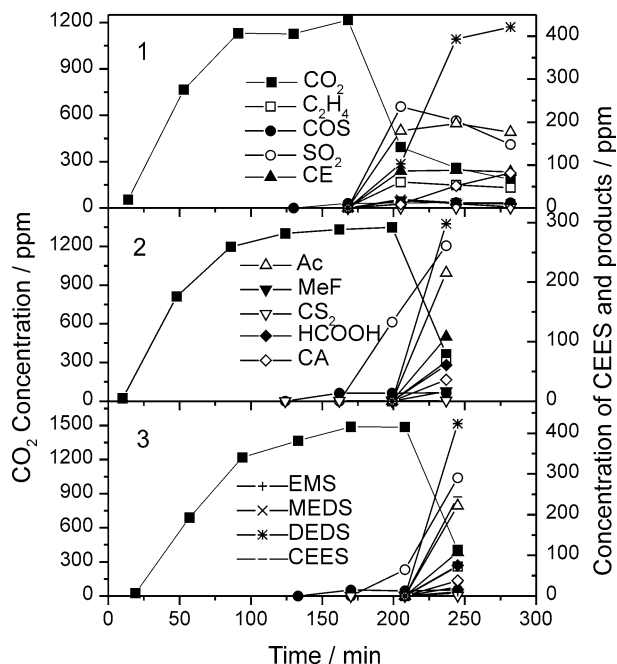

Fig. 3. Three consecutive runs of CEES photocatalytic oxidation at CEES feed concentration 807 ppm (30 μl/h liquid CEES), H_2O 1900 ppm, feed flow rate 130 cm^3/min. Product abbreviations are explained in Table 1.

ucts for mechanistic study. Profiles of effluent concentrations for twice-higher feed CEES concentrations are demonstrated in Fig. 1B. The rate of CEES injection into the air stream was kept the same as for Fig. 1A, but the air flow rate was decreased twice. It is surprising to note that the only detected product of incomplete oxidation in this case was carbonyl sulfide (COS) and its concentration was only a few ppm. However, COS appeared in the effluent earlier (360 min) which means quicker catalyst deactivation. At 525 min the CEES injection was ceased and further curves show oxidation of organics that were adsorbed onto the TiO_2 surface. Their oxidation finished in about 2000 min after the CEES injection had been stopped. The catalyst was reactivated thereafter by washing with purified water.

It is clear that only few intermediate products in small amounts are released from the coil reactor if it operates at a low CEES injection rate, irrespective of feed CEES concentration. Increasing the CEES injection rate by the factor of 2.5 led to the appearance of many by-products as two consecutive experiments in Fig. 2 show. After the CEES injection had been commenced, the reactor produced only CO_2 as the product for approximately 200 min. Then, the CO_2 concentration decreased abruptly and various products appeared in the effluent revealing the development of photocatalyst deactivation. All the detected gaseous products in this study, their abbreviations, and selectivities are summarized in Table 1. The main products of incomplete oxidation in Fig. 2 are acetaldehyde (Ac), SO_2, chloroethylene, and chloroacetaldehyde (CA). CEES appears at 380 min of reaction, that is, after ca. 180 min of the catalyst deactivation.
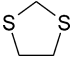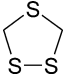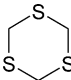
This deactivation behavior is very similar to that of diethyl sulfide [22]. The two parts of Fig. 2 represent consecutive runs under the same conditions. The photocatalyst was reactivated by irradiation in humidified air and washing with water. One can see that the time at which the CO_2 effluent concentration starts decreasing is the same for both runs. Thus, the photocatalyst was reactivated completely.

The same rate of CEES injection but under half the air flow rate was used for the experiments in Fig. 3. It is interesting to see that despite a twice-higher CEES feed concentration, the deactivation time remains about the same as in Fig. 2. The lower feed flow rate allowed detection of several minor gaseous intermediate products that are included in Table 1. Major gaseous products were acetaldehyde, SO_2, diethyl disulfide (DEDS). The three runs shown in Fig. 3 were performed consecutively in order to check for permanent photocatalyst deactivation. Such deactivation was observed previously for diethyl sulfide [22] and can be associated with photocatalyst etching by surface sulfuric acid. Between the runs, photocatalyst was reactivated by direct washing with acetonitrile and/or water. The coil reactor provides a good opportunity to study extractable products on a TiO_2 surface since they are accumulated in significant quantities and can be easily extracted without removing photocatalysts from the reactor. The three runs in Fig. 3 did not show permanent photocatalyst deactivation as the time of CO_2 concentration fall did not decrease. There even was some extension of deactivation time from the first to the third run.

Table 1
Gaseous products of CEES photocatalytic oxidation

No.	Name	Structure	Abbreviation	Maximum selectivity (Vol%)[a]
1	Carbon dioxide	CO_2	–	100
2	Ethylene	C_2H_4	–	2.8
3	Hydrogen sulfide	H_2S	–	0.4
4	Carbonyl sulfide	COS	–	1.5
5	Sulfur dioxide	SO_2	–	18
6	Chloroethylene	CH_2CHCl	CE	8
7	Acetaldehyde	CH_3CHO	Ac	38
8	Methyl formate	$HCOOCH_3$	MeF	1.1
9	Chloroethane	CH_3CH_2Cl	–	0.3
10	Carbon disulfide	CS_2	–	0.6
11	Ethyl formate	$HCOOCH_2CH_3$	EtF	0.9
12	Formic acid	HCOOH	–	4.3
13	Chloroacetaldehyde	$ClCH_2CHO$	CA	9.1
14	Ethyl methyl sulfide	$CH_3CH_2SCH_3$	EMS	4.8
15	Acetic acid	CH_3COOH	AcOH	7.9
16	Methyl ethyl disulfide	$CH_3CH_2SSCH_3$	MEDS	0.4
17	Diethyl disulfide	$CH_3CH_2SSCH_2CH_3$	DEDS	25
18	Hydrochloric acid	HCl	–	–
19	1,3-Dithiolane	(structure)	DTL	0.4
20	1,2,4-Trithiolane	(structure)	TTL	0.3
21	Chloroethyl ethyl disulfide	$ClCH_2CH_2SSCH_2CH_3$	CEED	5.8
22	1,3,5-Trithiane	(structure)	TTA	0.5
23	1,2-Bis(ethylthio)ethane	$C_2H_5SCH_2CH_2SC_2H_5$	BETE	0.8

[a] Among gaseous products listed in this table except hydrochloric acid.

3.2. Products of CEES photocatalytic degradation

Considering the gaseous products of CEES photocatalytic oxidation (Table 1) one can see that they do not differ principally from products of diethyl sulfide (DES) oxidation [22]. Such products as ethylene, carbonyl sulfide, SO_2, acetaldehyde, methyl formate, CS_2, formic acid, acetic acid, methyl ethyl disulfide, and diethyl disulfide were detected for both CEES and DES oxidation. The following products of CEES oxidation—chloroethylene, chloroacetaldehyde, and 2-chloroethyl ethyl disulfide—are analogous to corresponding products of DES oxidation without chlorine atoms. Some additional products of CEES oxidation were mostly generated with selectivity below 1% (Table 1). The exception is ethyl methyl sulfide that was not detected in gaseous DES oxidation products but was registered in surface products. This product should result from recombination of ethanethiyl and methyl radicals on the TiO_2 surface.

Less volatile products of CEES oxidation were studied by extracting them from the TiO_2 surface with dry acetonitrile. Previously, water was used for extraction of semivolatile products of DES oxidation [22]. However, CEES easily hydrolyses in water and many products are expected to react with water. Therefore, acetonitrile was used instead. Be-

fore GC-MS analysis, the hydrogen of hydroxyl groups in CEES products was substituted with a trimethylsilyl group to increase the products volatility and stability. The detected underivatized products are listed in Table 2. It should be emphasized that significant quantities of unreacted CEES were extracted after the reaction. No DES was extracted after the oxidation and it was not detected in the reactor effluent. Obviously CEES is less reactive in photocatalytic oxidation than DES due to the presence of electron-withdrawing chlorine atoms. Compared to products of DES oxidation, a much wider variety of products was detected for CEES. Hydroxyethyl ethyl sulfide was formed in the hydrolysis of CEES. The main surface product was 2-chloroethyl ethyl sulfoxide. Though ethanesulfinic acid was detected in significant quantities in the acetonitrile catalyst extract, the corresponding ethanesulfonic acid was detected only in water catalyst extract. The ethanesulfonic acid was adsorbed strong enough so that acetonitrile could not extract it. Ethyl vinyl sulfide and ethyl vinyl sulfoxide were minor products in acetonitrile wash. Other products can be classified as mono and disubstituted in the β position with chlorine and hydroxyl group disulfides, thiosulfonates, trisulfides, and tetrasulfides. Corresponding unsubstituted sulfides were detected in DES oxidation products [22]. Therefore, the introduction of chlorine atoms into diethyl sulfide decreased reactivity but did

Table 2
Compounds extracted from the TiO_2 surface with acetonitrile after CEES photocatalytic oxidation

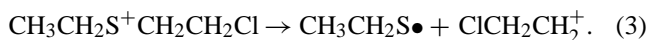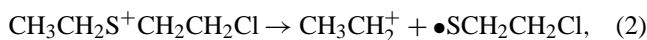| No.	Name	Structure	Content (%)
1	2-Chloroethanol	$ClCH_2CH_2OH$	0.5
2	Ethyl vinyl sulfide	$CH_2CHSCH_2CH_3$	0.8
3	Bis(2-chloroethyl)sulfide	$ClCH_2CH_2SCH_2CH_2Cl$	0.4
4	2-Chloroethyl ethyl sulfide (CEES)	$ClCH_2CH_2SCH_2CH_3$	32
5	Ethyl vinyl sulfoxide	$CH_3CH_2S(O)CHCH_2$	0.3
6	Ethanesulfinic acid	$CH_3CH_2SO_2H$	2.0
7	Hydroxyethyl ethyl sulfide (HEES)	$HOCH_2CH_2SCH_2CH_3$	1.4
8	Hydroxyacetic acid	$HOCH_2COOH$	0.7
9	Unknown MW 192		0.5
10	2-Chloroethyl ethyl disulfide	$ClCH_2CH_2SSCH_2CH_3$	4.3
11	Diethyl trisulfide	$CH_3CH_2SSSCH_2CH_3$	1.0
12	Diethyl thiosulfonate	$CH_3CH_2SS(O_2)CH_2CH_3$	2.0
13	2-Chloroethyl ethyl sulfoxide	$ClCH_2CH_2S(O)CH_2CH_3$	21
14	2-Hydroxyethyl ethyl disulfide	$HOCH_2CH_2SSCH_2CH_3$	0.6
15	2-Hydroxyethyl ethyl sulfoxide	$HOCH_2CH_2S(O)CH_2CH_3$	1.2
16	2-Chloroethyl ethyl trisulfide	$ClCH_2CH_2SSSCH_2CH_3$	3.1
17	Bis(2-chloroethyl) disulfide	$ClCH_2CH_2SSCH_2CH_2Cl$	14
18	2-Chloroethyl ethyl thiosulfonate	$ClCH_2CH_2SS(O_2)CH_2CH_3$	2.7
19	2-Hydroxyethyl ethyl trisulfide	$HOCH_2CH_2SSSCH_2CH_3$	0.2
20	2-Hydroxyethyl-2′-chloroethyl disulfide	$HOCH_2CH_2SSCH_2CH_2Cl$	2.2
21	Chloroethyl dichloroethyl disulfide	$ClCH_2CH_2SSC_2H_3Cl_2$	0.3
22	2-Hydroxyethyl ethyl thiosulfonate	$HOCH_2CH_2SS(O_2)CH_2CH_3$	0.3
23	2-Chloroethyl ethyl tetrasulfide	$ClCH_2CH_2SSSSCH_2CH_3$	0.5
24	Bis(2-chloroethyl) trisulfide	$ClCH_2CH_2SSSCH_2CH_2Cl$	5.5
25	2-Hydroxyethyl-2′-chloroethyl trisulfide	$HOCH_2CH_2SSSCH_2CH_2Cl$	0.6
26	Bis(2-chloroethyl) tetrasulfide	$ClCH_2CH_2SSSSCH_2CH_2Cl$	0.8

Content was calculated from peak areas.

not change the routes of photocatalytic transformation. Since significant amounts of organic products are accumulated on the TiO_2 surface, they can contribute to catalyst deactivation. This was indirectly corroborated by disproportionately faster deactivation at higher DES concentrations [22].

There is a possibility that some products of CEES oxidation were formed in a dark process. To check such reactions, a blank experiment was performed under the same conditions as in Fig. 3 but without ultraviolet irradiation of photocatalyst. Neither any of the products nor CEES were detected for about 200 min of the experiment. Then, the concentration of CEES in the reactor effluent began to grow gradually due to saturation of surface adsorption sites. Thus, gaseous products are not formed in the dark. However, some surface products can be generated. The surface products were extracted with acetonitrile and derivatized with trimethylsilyl groups. The identified products of the dark CEES reaction over TiO_2 are listed in Table 3. The major product was 2-hydroxyethyl ethyl sulfide that is formed from CEES by hydrolysis. Bis(ethylthio)ethane was also detected but in a quantity close to its content in the starting CEES. Other compounds could be the dark products but were present in very small amounts. Therefore, the dark reaction gives significant contribution only to hydrolysis of CEES. It is interesting to note that the percentage content of 2-hydroxyethyl ethyl sulfide is much higher in the dark than in the light. It means a much higher photocatalytic reactivity of 2-hydroxyethyl ethyl sulfide compared to CEES.

3.3. Mechanism of CEES photocatalytic degradation

Significant amounts of chlorine-containing products as well as a high content of CEES on the TiO_2 surface after the dark reaction signify that a big fraction of CEES takes part in photocatalytic reactions before it hydrolyses. Photocatalytic oxidation of organic sulfides starts with sulfur radical cations [1, 3, 5, etc.]. Further, the radical cation of CEES includes reaction with oxygen or superoxide ions to form sulfone, which is converted to sulfoxide via the reaction with another CEES molecule [20]. The radical cation can also undergo cleavage of either of C–S bonds

$$CH_3CH_2S^+CH_2CH_2Cl \rightarrow CH_3CH_2^+ + \bullet SCH_2CH_2Cl, \quad (2)$$

$$CH_3CH_2S^+CH_2CH_2Cl \rightarrow CH_3CH_2S\bullet + ClCH_2CH_2^+. \quad (3)$$

The alkyl cations can react with water to produce the corresponding alcohols—ethanol and 2-chloroethanol. Ethanol was not detected in the present study, but was registered in the oxidation of diethyl sulfide [20]. 2-Chloroethanol was detected in the present work in extracts from the TiO_2 surface. Another transformation route of alkyl radical cations is proton elimination. This reaction should be assisted by a base that can be superoxide anions. The proton elimination will produce ethylene and chloroethylene, both products having been registered in this study. The thiyl radicals $CH_3CH_2S\bullet$ and $\bullet SCH_2CH_2Cl$ will recombine in all possible combinations giving the detected products diethyl disulfide, 2-chloroethyl ethyl disulfide, and bis(2-chloroethyl)

Table 3
Compounds extracted from the TiO$_2$ surface with acetonitrile after dark CEES purging

| No.	Name	Structure	Content (%)
1	2-Chloroethyl ethyl sulfide (CEES)	ClCH$_2$CH$_2$SCH$_2$CH$_3$	81.7
2	2-Hydroxyethyl ethyl sulfide	HOCH$_2$CH$_2$SCH$_2$CH$_3$	17.8
3	Ethanesulfinic acid	CH$_3$CH$_2$SO$_2$H	0.04
4	Bis(2-chloroethyl)sulfide	ClCH$_2$CH$_2$SCH$_2$CH$_2$Cl	0.06
5	Bis(ethylthio)ethane	CH$_3$CH$_2$SCH$_2$CH$_2$SCH$_2$CH$_3$	0.3
6	2-Chloroethyl ethyl sulfoxide	ClCH$_2$CH$_2$S(O)CH$_2$CH$_3$	0.07
7	Bis(2-(ethylthio)ethyl) ether	(CH$_3$CH$_2$SCH$_2$CH$_2$)$_2$O	0.03
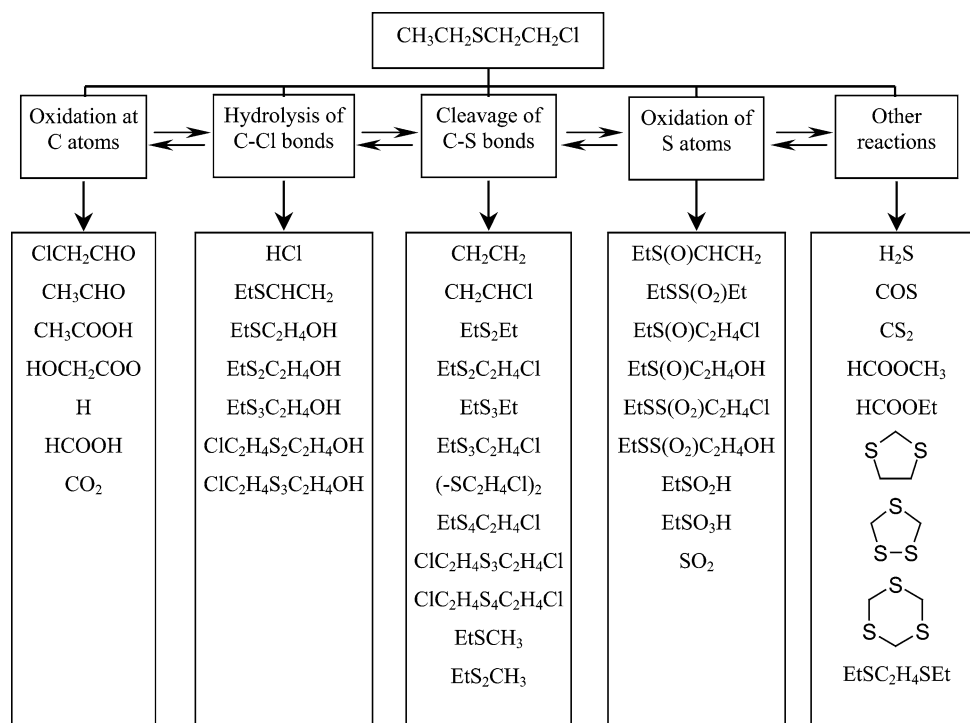
Fig. 4. Major routes of CEES photocatalytic oxidation.

disulfide. The disulfides in turn will interact with photo-generated holes and undergo reactions similar to CEES radical cations. The corresponding radicals CH$_3$CH$_2$SS• and •SSCH$_2$CH$_2$Cl will recombine with each other and the above thiyl radicals giving detected tetrasulfides and trisulfides.

The possible involvement of α-C–H bond deprotonation in CEES gas-phase photocatalytic oxidation cannot be concluded from large amounts of produced acetaldehyde and chloroacetaldehyde because these products are easily formed in the oxidation of ethanol and chloroethanol, respectively. Small amounts of alcohols can be associated with higher selectivity to oxidation of alcohols compared to aldehydes as was demonstrated for ethanol [25]. The transformations of CEES are schematically summarized in Fig. 4. It should be noted that the mechanism is highly cross-linked and various stages can follow in complex combinations.

3.4. TiO$_2$ deactivation/reactivation studied by FTIR technique

The design of the coil reactor did not allow direct studying of the photocatalyst surface by FTIR methods. Therefore, the surface processes were investigated over TiO$_2$ deposited onto a BaF$_2$ in a flow reactor. Before FTIR photocatalytic experiments, the FTIR spectrum of the gaseous starting CEES was taken in a gas cell. The spectrum was very close to a published spectrum [26]. The assignment of the observed bands is given in Table 4. The most intensive bands are observed in the region of C–H stretching vibrations 2880–2970 cm^{-1}. The band 1454 cm^{-1} is attributed to merged bands of C–H asymmetric vibrations in CH$_3$ and CH$_2$Cl groups and scissor vibrations of CH$_2$ groups. The less intensive band at 1385 cm^{-1} corresponds to CH$_3$ symmetrical deformation vibration. The 1270 cm^{-1} band is ascribable to CH$_2$ wagging in the CH$_2$Cl group since the CH$_2$–Hal group is known to possess such an intensive band

Table 4
Assignment of bands in FTIR spectra

| Bands (cm^{-1})	Assignment	References
1634 wide	Adsorbed H_2O, $\delta(H_2O)$	[27,28]
3240 wide	Adsorbed H_2O, $\nu(O-H)$	[27,28]
2970 ± 10	C–H vibrations—$\nu_{AS}(CH_3)$, $\nu_{AS}(CH_2Cl)$	[27,28]
2936 ± 5	C–H vibrations—$\nu_{AS}(CH_2S)$	[27,28]
2880 ± 5	C–H vibrations—$\nu_S(CH_3)$, $\nu_S(CH_2Cl)$, $\nu_S(CH_2S)$	[27,28]
1454	C–H vibrations—$\delta_{AS}(CH_3)$, $\delta(CH_2)$, $\delta(CH_2Cl)$	[27,28]
1382 ± 3	C–H vibrations—$\delta_S(CH_3)$	[27,28]
1271	CH_2 wagging in CH_2Cl in CEES	[27]
1215	CH_2 wagging in CH_2S in CEES	[27]
1269	$\delta(OH)$ in CH_2OH	[27,28]
1055	$\nu(C-O)$ in CH_2OH	[27,28]
1724	$\nu(C=O)$ in COOH, R_2CO	[27,28]
1550, 1580	$\nu_{AS}(COO^-)$	[27,29]
1416	$\nu_S(COO^-)$	[27,29]
1250	$\nu_{AS}(SO_3^-)$ in RSO_3^-	[27]
1042	$\nu_S(RSO_3^-)$ in RSO_3^-, $\nu(SO)$ in R_2SO	[27]
1133 ± 5, 1042	Adsorbed monodentate SO_4^{2-}	[29]
995, 1065, 1126, 1200	Adsorbed bidentate SO_4^{2-}	[29]
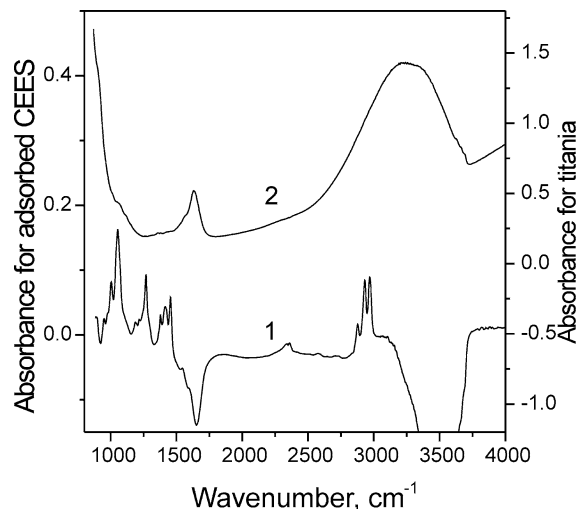
Fig. 5. FTIR spectra of CEES adsorbed on TiO_2 surface after subtraction of the spectrum of the initial TiO_2 (1) and initial TiO_2 before the admission of CEES(2).

at 1240–1300 cm^{-1} [27]. The band at 1215 cm^{-1} should correspond to CH_2 wagging of the CH_2–S group; the range for the strong band of such vibrations is 1220–1270 cm^{-1}.

Curve 2 in Fig. 5 demonstrates the transmission spectrum of the TiO_2 before any adsorption and photocatalytic experiments. The wide band at 3240 cm^{-1} is due to O–H stretching vibrations of physisorbed and chemisorbed water. One can see small shoulders in the high-frequency region that correspond to surface OH groups. The deformation vibrations of water are observed at 1634 cm^{-1}. At wavenumbers below 1000 cm^{-1}, the strong absorption starts due to lattice vibrations of TiO_2. This spectrum of the starting TiO_2 was subtracted from all the spectra reported below.

Curve 1 in Fig. 5 corresponds to subtracted spectrum obtained after 2 h of adsorption of CEES on the TiO_2/BaF_2 sample in the flow reactor. The negative bands of adsorbed

water at 1600 and 3500 cm^{-1} show that CEES effectively displaces water from the TiO_2 surface. The spectrum differs markedly from the spectrum of gaseous CEES. Comparison with spectra in a FTIR spectra library [26] shows that the spectrum obtained after adsorption of CEES is similar to the spectrum of condensed HEES. The bands 1454 and 1379 cm^{-1} belong to deformation vibrations of CH_3 and CH_2 groups whereas the band 1416 cm^{-1} should be attributed to deformation vibrations in the CH_2OH group. Band 1269 cm^{-1} is attributable to deformation vibrations of the OH group in the CH_2OH fragment [27], and the band at 1055 cm^{-1} belongs to the region of 1030–1085 cm^{-1} of C–O stretching vibrations in primary alcohols [27]. The absence of the bands of CEES testifies to the hydrolysis of the majority of CEES on the TiO_2 surface. However, the spectrum in Fig. 5 does not preclude the possibility that some part of CEES stays on the TiO_2 surface. The characteristic bands of CEES at 1271 and 1215 cm^{-1} can be masked by the wide band of HEES at 1269 cm^{-1}.

The surface changes in deactivation were studied in a separate experiment over the fresh TiO_2/BaF_2 sample. At the start of experiment CEES supply and UV light were turned on. Fig. 6 reveals the changes in substracted FTIR spectra with experiment time. Spectrum 1 was taken before the catalyst deactivated toward complete mineralization into CO_2. It shows very small bands in the region of C–H stretching vibrations, a small band at 1724 cm^{-1} in the region of ketones and aldehydes C=O stretching vibrations, a prominent band 1580 cm^{-1} that is attributable to asymmetric stretching vibrations of carboxylic acids [29]. The region 1200–1500 cm^{-1} contains many overlapping bands, among which the band 1250 cm^{-1} is distinguishable that corresponds to asymmetric stretching vibrations of sulfonic acids [27]. The bands 1040 and 1133 cm^{-1} belong to vibrations of monodentate sulfate. The band 1040 cm^{-1} also includes symmetric vibrations of sulfonic acids.
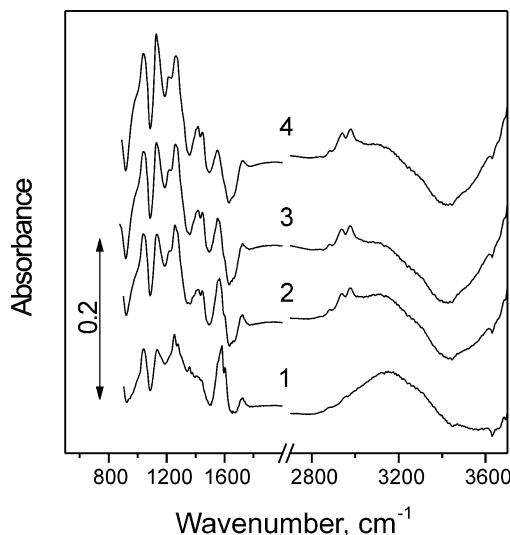
Fig. 6. FTIR spectra of species on the TiO_2 surface after CEES photocatalytic oxidation for 35 min (1), 70 min (2), 105 min (3), and 160 min (4).

After about 1 h of reaction, the catalyst deactivated for CO_2 evolution. Spectrum 2 in Fig. 6 shows corresponding changes in surface composition. The bands in the C–H stretching region show significant intensity and match mostly to adsorbed HEES. Upon further catalyst deactivation shown in spectra 2, 3, and 4 the intensity of C–H stretching bands increases, which corresponds to accumulation of surface HEES. The band of asymmetric stretching vibrations of a carboxyl group decreases, which should be associated with gradual oxidation of such species to CO_2. The rising bands around 1415 and 1450 cm^{-1} should be attributed to the C–H deformation vibrations of adsorbed HEES and products. The band at 1260 cm^{-1} increases and belongs to deformation vibrations of the OH group in CEES as well as asymmetric stretching vibrations of sulfonic acids. Finally, the bands 1040 and 1130 cm^{-1} corresponding to bisulfate species intensified, demonstrating, despite deactivation to evolution of gaseous CO_2, the oxidation of sulfur continued and proceeded to surface sulfate species.

One of the methods to partially reactivate the TiO_2 deactivated in sulfur compounds oxidation is irradiation in humidified air in the absence of organic compounds [22]. Spectra 1–5 in Fig. 7 demonstrate the evolution of a TiO_2 surface in the course of such reactivation. One can see that the bands of organic compounds gradually disappear and the bands of surface monodentate sulfates increase in intensity. Despite that organic material is mineralized and removed from the TiO_2, the surface sites mostly stay occupied with sulfates. Washing with water was used in order to remove the surface sulfates. Spectrum 6 in Fig. 7 demonstrates the TiO_2 surface composition after such reactivation procedure. The observed band with several shoulders and a summit at 1126 cm^{-1} corresponds to surface bidentate sulfate species [29]. The monodentate sulfate species were removed during the washing as sulfuric acid. Obviously, bidentate species are strongly bound to the TiO_2 surface that
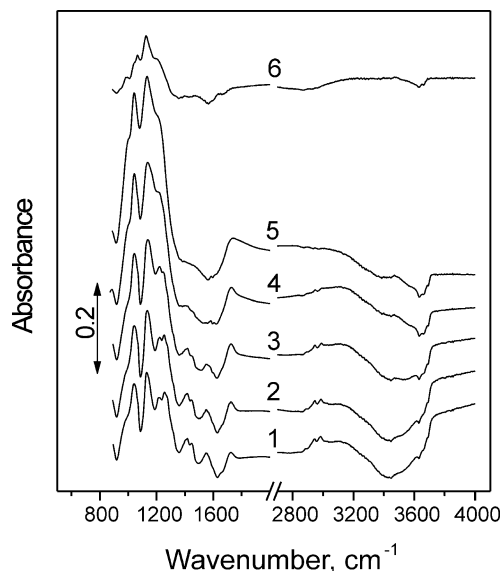

Fig. 7. FTIR spectra of species on the TiO_2 surface after irradiation of deactivated TiO_2 for 60 min (1), 120 min (2), 180 min (3), 285 min (4), 1205 min (5), and after washing the TiO_2 with clean water (6).

prevents their effective removal by washing. Accumulation of such surface species could contribute to the development of permanent deactivation of TiO_2 [22].

4. Conclusions

Toxic mustard gas imitant 2-chloroethyl ethyl sulfide undergoes mineralization in the gas-phase coil photocatalytic reactor but deactivates the TiO_2 photocatalyst. After deactivation, volatile by-products of the reaction are detectable in the reactor effluent and nonvolatile products accumulate on the TiO_2 surface. Only few by-products in low concentrations can be seen if the reactor operates at low CEES concentrations and low flow rates. The photocatalyst can be completely reactivated by washing with water. CEES showed decreased reactivity compared to its unchlorinated analog diethyl sulfide. The detected volatile and extracted from surface products of CEES degradation imply the main stages of reaction—oxidation of sulfur atoms and S–C bond cleavage accompanied by hydrolysis and followed by oxidation of carbon atoms. After deactivation to mineralization of carbonaceous species, oxidation of sulfur continues and results in surface monodentate sulfates. Washing with water removes these sulfates and leaves on the surface small quantities of bidentate sulfate species that may be responsible for enhanced photocatalytic activity in consecutive runs.

References

[1] R.S. Davidson, J.E. Pratt, Tetrahedron Lett. 52 (1983) 5903–5906.

[2] Y.-C. Yang, Photocatalytic Oxidation of Mustard Using Semiconductor Oxides, CRDEC, 1989, pp. 83–89.

[3] M.A. Fox, A.A. Abdel-Wahab, J. Catal. 126 (1990) 693–696.

[4] M.A. Fox, Y.-S. Kim, A.A. Abdel-Wahab, Catal. Lett. 5 (1990) 369–376.

[5] M.A. Fox, A.A. Abdel-Wahab, Tetrahedron Lett. 31 (1990) 4533–4536.

[6] C.-Y. Wang, C.-Y. Liu, T. Shen, J. Photochem. Photobiol. A 109 (1997) 65–70.

[7] E. Baciocchi, C. Crescenzi, O. Lanzalunga, Tetrahedron 53 (1997) 4469–4478.

[8] E. Baciocchi, T.D. Giacco, M.I. Ferrero, C. Rol, G.V. Sebastiani, J. Org. Chem. 62 (1997) 4015–4017.

[9] N. Somasundaram, C. Srinivasan, J. Photochem. Photobiol. A 115 (1998) 169–173.

[10] A.A. Abdel-Wahab, A.E. Gaber, J. Photochem. Photobiol. A 114 (1998) 213–218.

[11] M.H. Habibi, S. Tangestaninejad, B. Yadollahi, Appl. Catal. B 33 (2001) 57–63.

[12] M. Sokmen, D.W. Allen, A.T. Hewson, M.R. Clench, J. Photochem. Photobiol. A 141 (2001) 63–67.

[13] S. Matsuzawa, J. Tanaka, S. Sato, T. Ibusuki, J. Photochem. Photobiol. A 149 (2002) 183–189.

[14] Y. Shiraishi, T. Hirai, I. Komasawa, J. Chem. Eng. Jpn. 35 (2002) 489–492.

[15] N. Somasundaram, C. Srinivasan, Ind. J. Chem. B 41 (2002) 1523–1525.

[16] A.V. Vorontsov, A.A. Panchenko, E.N. Savinov, P.G. Smirniotis, Environ. Sci. Technol. 36 (2002) 5261–5269.

[17] J. Peral, D.F. Ollis, J. Mol. Catal. A 115 (1997) 347–354.

[18] M.C. Canela, R.M. Alberici, M.N. Eberlin, W.F. Jardim, Environ. Sci. Technol. 33 (1999) 2788–2792.

[19] M.C. Canela, R.M. Alberici, W.F. Jardim, J. Photochem. Photobiol. A 112 (1998) 73–80.

[20] A.V. Vorontsov, E.N. Savinov, L. Davydov, P.G. Smirniotis, Appl. Catal. B 32 (2001) 11–24.

[21] D.V. Kozlov, A.V. Vorontsov, P.G. Smirniotis, E.N. Savinov, Appl. Catal. B 42 (2003) 77–87.

[22] A.V. Vorontsov, E.N. Savinov, C. Lion, P.G. Smirniotis, Appl. Catal. B 44 (2003) 25–40.

[23] A.V. Vorontsov, L. Davydov, E.P. Reddy, C. Lion, E.N. Savinov, P.G. Smirniotis, New J. Chem. 26 (2002) 732–744.

[24] F.W. McLafferty, F. Tureček, Interpretation of Mass Spectra, Univ. Science Books, Sausalito, CA, 1993.

[25] A.V. Vorontsov, E.N. Savinov, G.B. Barannik, V.N. Troitsky, V.N. Parmon, Catal. Today 39 (1997) 207–218.

[26] C.J. Pouchert, The Aldrich library of FT-IR spectra, Aldrich Chem. Co., 1985.

[27] G. Socrates, Infrared Characteristic Group Frequencies, Wiley, New York, 1994.

[28] Handbook of Chemistry and Physics, 56th ed., CRC Press, Boca Raton, FL, 1975–1976.

[29] K. Nakamoto, Infrared and Raman Spectra of Inorganic and Coordinated Compounds, Wiley, New York, 1986.